



Effects of Sediment Characteristics on Carbon Dioxide Fluxes Based on Interacting Factors in Unvegetated Tidal Flats

Wei-Jen Lin^{1,2}, Ming-Chih Chiu^{1,2}, Chiao-Wen Lin^{1,2} and Hsing-Juh Lin^{1,2*}

¹ Department of Life Sciences, National Chung Hsing University, Taichung, Taiwan, ² Innovation and Development Center of Sustainable Agriculture, National Chung Hsing University, Taichung, Taiwan

OPEN ACCESS

Edited by:

Wen-Chen Chou,
National Taiwan Ocean University,
Taiwan

Reviewed by:

Dominique Davoult,
Sorbonne Université, France
Wei-Jen Huang,
National Sun Yat-sen University,
Taiwan

*Correspondence:

Hsing-Juh Lin
hjlin@dragon.nchu.edu.tw

Specialty section:

This article was submitted to
Marine Ecosystem Ecology,
a section of the journal
Frontiers in Marine Science

Received: 20 February 2021

Accepted: 19 April 2021

Published: 17 May 2021

Citation:

Lin W-J, Chiu M-C, Lin C-W and
Lin H-J (2021) Effects of Sediment
Characteristics on Carbon Dioxide
Fluxes Based on Interacting Factors
in Unvegetated Tidal Flats.
Front. Mar. Sci. 8:670180.
doi: 10.3389/fmars.2021.670180

The contribution of unvegetated tidal flats to global net primary production is comparable to that of some vegetated coastal habitats. However, compared to carbon flux regulating factors in vegetated habitats, those in unvegetated tidal flats are not well understood, particularly in terms of their cause-effect relationships. Maximum gross primary production (GPP_m), net primary production (NPP) and total respiration (TR) during emersion at noon when the irradiance level was at the saturation level for photosynthesis in nine unvegetated tidal flats across the Taiwan Strait in tropical and subtropical regions were determined in winter and summer from 2011 to 2016 to examine the direct and indirect relationships between sediment characteristics and carbon fluxes by using structural equation models (SEM). Most of the GPP_m and NPP values were higher in winter than in summer. Conversely, the TR values were higher in summer than in winter. The NPP values at some sites shifted to negative values in summer, indicating the sites were carbon sources. The values of GPP_m , TR and NPP for the tidal flats all increased significantly with increasing sediment mud content. The SEM results showed that the sediment mud content directly increased GPP_m or indirectly increased GPP_m via a compositional shift in benthic microalgae. The sediment mud content also directly increased TR or indirectly increased TR via increased organic matter content. The contribution of benthic microalgal and macrofaunal biomass to TR was relatively minor. This result suggests that primary production was stimulated mainly by the organic matter content rather than by increased microalgal biomass. With the integrated SEM framework, our results showed mechanistic evidence of how sediment mud content acted as a critical factor regulating carbon fluxes in unvegetated tidal flats.

Keywords: benthic metabolism, gross primary production, net primary production, respiration, microphytobenthos, structural equation model

INTRODUCTION

Unvegetated tidal flats (hereafter tidal flats) are the area inundated between the high- and low-tide waterlines, including sandy and muddy sediments (Murray et al., 2012). Tidal flats encompass a large proportion of the coastal zone. The global area of tidal flats has been estimated at 127,921 km², with most being distributed in Asia (44% of total; Murray et al., 2019). The estimated global area

of tidal flats is only 16% of that of seagrass beds but is comparable to that of mangroves and 2.3 times that of salt marshes (Davidson and Finlayson, 2019). Although the daily rate of net primary production (NPP) in tidal flats is at most 20% of that of vegetated coastal habitats, the global NPP of tidal flats ($11.04 \text{ Tg C yr}^{-1}$), obtained by multiplying the NPP by the global area, might reach approximately 50% of that of salt marshes (Lin et al., 2020). The carbon stock of tidal flats (78.07 Tg C) is nearly four times higher than that of vegetated habitats (20.53 Tg C) along the coast of China (Chen et al., 2020). Currently, anthropogenic activities, such as land development (Koh and Khim, 2014; Chen et al., 2016), oil spills (Junoy et al., 2005; Lee and Lin, 2013; Yu et al., 2013) and heavy metal pollution (Rahman and Ishiga, 2012; Zhang et al., 2013), tend to occur in tidal flats.

Benthic microalgae, also known as microphytobenthos, are generally the major primary producers in tidal flats throughout the year (McIntyre et al., 1996; Underwood and Kromkamp, 1999). These microalgae can contribute up to 65% of the combined production of phytoplankton and benthic microalgae in shallow-water ecosystems (McMinn et al., 2005; Sarker et al., 2009). This production can provide food sources for not only local benthic systems but also nearby pelagic systems. Over 30% of benthic microalgae may be resuspended by the turbulence of tidal currents and wind-generated waves (De Jonge and Van Beuselum, 1992), part of which is exported to nearby coastal ecosystems by tidal currents and further subsidizes secondary production through the outwelling of benthic microalgae (Guarini et al., 2008; Yoshino et al., 2012; Savelli et al., 2019).

The production of benthic microalgae in tidal flats is frequently higher in tropical regions than in temperate regions (Cahoon, 1999). In temperate regions, tidal flats might be either small carbon sinks or carbon sources during emersion (Brotas and Catarino, 1995; Migné et al., 2004; Hubas and Davoult, 2006; Spilmont et al., 2006; Otani and Endo, 2019). In subtropical regions, tidal flats act as carbon sinks during emersion (Lee et al., 2011). Lin et al. (2020) demonstrated a clear latitudinal gradient in winter from 20°N to 40°N in which primary production and respiration in tidal flats during emersion decreased by up to 104% toward higher latitudes, but no clear trend was detected across the latitudinal gradient in summer. It appears that the contribution of NPP from tidal flats to the coastal carbon flux was greater in tropical and subtropical regions than in temperate regions (Lin et al., 2020). Along the latitudinal gradient, sediment temperature is a main factor that regulates carbon fluxes in tidal flats (Lin et al., 2020). The authors also indicated that sediment features might be more prominent in regulating carbon fluxes in tidal flats at a local scale. However, both direct and indirect relationships between sediment characteristics and carbon fluxes in tidal flats are rarely emphasized simultaneously.

There is still no comprehensive quantitative analysis addressing the network of relationships between sediment characteristics and carbon fluxes from benthic microalgae. Some studies have reported no clear relationship between sediment characteristics and the production of benthic microalgae (Davis and McIntire, 1983; Hubas et al., 2006). Others have suggested a negative relationship between sediment mud content and

benthic production (Billerbeck et al., 2007; Lee et al., 2011). However, some studies have noted that benthic production was higher in sediments with higher mud content (Colijn and de Jonge, 1984; Hubas et al., 2007; Davoult et al., 2009; Migné et al., 2016; Haro et al., 2020). This inconsistency might be due to different study scales. Most studies have measured only one tidal flat with a limited number of sampling sites; few studies, however, have measured different tidal flats representing a gradient of sediment characteristics. For example, Pratt et al. (2014) compiled data on gross primary production (GPP) and sediment oxygen consumption from nine intertidal flats on the North Island of New Zealand and found that both processes decreased with increases in sediment mud content. However, the range of sediment mud content was between 0 and 30%. It is uncertain whether benthic metabolism would respond in the same way to sediment with mud content $> 30\%$. In this study, because primary production of benthic microalgae mostly occurs on the surface of tidal flats during daytime emersion (Lee et al., 2011), we determined the carbon dioxide (CO_2) fluxes in nine tidal flats during emersion in tropical and subtropical regions along a larger gradient of sediment mud content, between 0 and 90% in summer and winter, respectively. It was hypothesized that the CO_2 fluxes in tidal flats would decrease with increasing sediment mud content. We further explored multiple hypotheses about the direct and indirect relationships between CO_2 fluxes in tidal flats and sediment characteristics by using structural equation models (SEM).

MATERIALS AND METHODS

Sampling Sites

Nine tidal flats in tropical and subtropical regions across the Taiwan Strait (22.48°N – 26.15°N) were chosen as our sampling sites in this study. Five of the sites were in the eastern Taiwan Strait, and four of the sites were located in the western Taiwan Strait (Figure 1 and Table 1). Measurements at each site were conducted separately in summer and in winter. Due to labor constraints and financial difficulties, all the measurements were not necessarily conducted in the same year. The air temperature ranges from 11.2 to 20.0°C in winter and from 27.1 to 30.0°C in summer. The annual precipitation ranges from 908 to 1735 mm. The climate data in the studied years were derived from the local weather station at each sampling site and obtained from the Observation Data Inquiry System of the Central Weather Bureau, Taiwan¹.

Carbon Flux Measurements

The carbon fluxes in the tidal flats were measured during emersion at each sampling site by the benthic closed-chamber method. This method, which was originally developed by Migné et al. (2002) and modified by Lee et al. (2011), was used to measure CO_2 fluxes from the sediment through the photosynthesis of benthic microalgae and through autotrophic and heterotrophic respiration (i.e., total respiration) within the

¹<https://e-service.cwb.gov.tw/HistoryDataQuery>

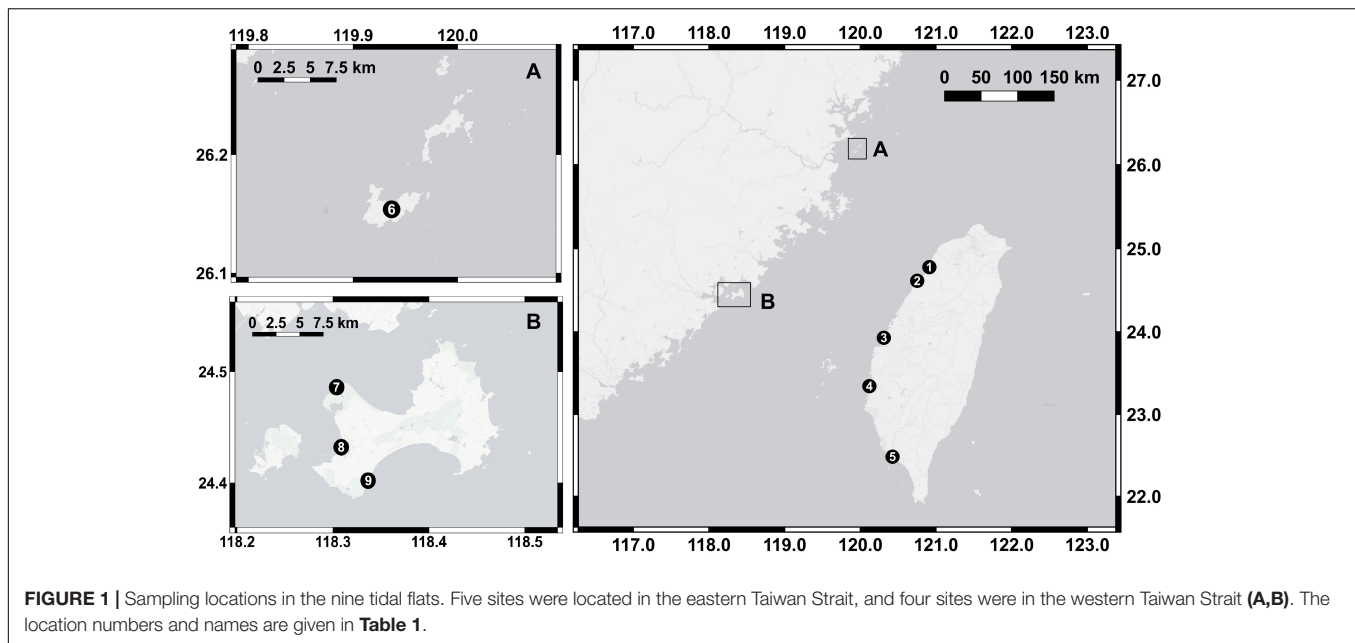


TABLE 1 | Locations, study years, and meteorological conditions in the tidal flats.

Site	Latitude, longitude	Studied years	Air temperature (°C)		Annual precipitation (mm)	
			Winter	Summer		
#1	Siangshan (SS)	24.778°N, 120.913°E	2011~2012	15.3	28.3	1664
#2	Houlong (HL)	24.614°N, 120.752°E	2014~2016	15.7	28.7	1502
#3	Fangyuan (FY)	23.928°N, 120.311°E	2014~2016	17.1	28.8	1160
#4	Haomeiliao (HML)	23.343°N, 120.120°E	2015~2016	18.3	30.0	1735
#5	Gaoping (GP)	22.484°N, 120.426°E	2014~2016	20.0	28.9	2108
#6	Nangan (NG)	26.153°N, 119.937°E	2014	11.2	27.1	908
#7	Beishan (BS)	24.485°N, 118.303°E	2011, 2013	13.4	27.6	1091
#8	Wujiang (WJ)	24.415°N, 118.308°E	2011, 2013	13.4	27.6	1091
#9	Oucuo (OC)	24.401°N, 118.336°E	2011, 2013	13.4	27.6	1091

The air temperature in winter and in summer and the annual precipitation were averaged when the study took place over more than one year. The meteorological data are available at <https://e-service.cwb.gov.tw/HistoryDataQuery>.

chamber. Measurements were conducted *in situ* on sunny days under ambient light conditions at noon (10:00 to 14:00) because the irradiance level was at the saturation level for photosynthesis. The respiration in subtropical tidal flats during nighttime was 50% lower than that during daytime (Lee et al., 2011). However, the main purpose of this study was to examine the relationships between sediment characteristics and carbon fluxes rather than quantifying daily production in the tidal flats. Since the CO₂ fluxes might be affected by tides (Spilmont et al., 2007), emersions during spring tides were selected as the measurement times at all sampling sites to enable cross-site comparisons.

During emersion, a benthic chamber, composed of a semicircular transparent acrylic dome on the top and a stainless steel ring (30 cm in diameter and 16 cm in height) at the bottom, were pushed into the sediment of tidal flats to a depth of 10 cm. The chamber encompassed 10.6 L of air over a sediment area of 0.071 m² within the dome. To make the chamber airtight, gas leakage was always excluded prior to

each measurement. CO₂ fluxes between the sediment and the air were monitored by an infrared CO₂ gas analyzer (LI-820, LI-COR, Lincoln, NE, United States) and recorded by a data logger (LI-1400, LI-COR) with a 30 s logging frequency for 10 min before the environmental conditions (i.e., air pressure, temperature, and humidity) obviously increased within the chamber compared to outside conditions. The CO₂ fluxes (in mg C m⁻² h⁻¹) were calculated by the slope of the linear regression line between CO₂ concentration (ppm) and recorded frequency (30 s), assuming a molar volume of 24.5 L mol⁻¹ at normal temperature (25°C) and pressure (1 atm) (NTP) and a molar mass of 12 g C mol⁻¹ CO₂. To avoid any potential perturbation during initial measurements, only CO₂ fluxes during the last 8 min were regressed against time. The linear regressions were acceptable when the determination coefficient was >0.80. Photosynthetically active radiation (PAR, 400–700 nm, in μmol quanta m⁻² s⁻¹) and sediment temperature were recorded simultaneously outside the chamber with a quantum sensor

(LI-190SA, LI-COR) and a temperature sensor (LI-1400-101, LI-COR) with the same data logger listed above.

On each measurement, three to five benthic chambers were used. These benthic chambers were placed on the sediment approximately 5 m apart to eliminate any potential interactions between the sediment samples. We performed the measurements on separate days to collect sufficient replicates in each season for each site (Table 2). Prior to each measurement, the CO₂ gas analyzers were calibrated with CO₂-free gas and 500 ppm CO₂. The accuracy of the CO₂ gas analyzer was <2.5% of the measurement.

The measurements under ambient light conditions allowed us to estimate the NPP, and the measurements performed in the dark (100% shading) allowed the estimation of total respiration (TR). The GPP describes the total uptake of CO₂ by a tidal flat, which was calculated by adding the NPP to the TR as shown in Equation (1).

$$\text{GPP} = \text{NPP} + \text{TR} \quad (1)$$

whenever the sum of NPP and TR was negative, the tidal flat showed heterotrophic conditions; the GPP was then assumed to be zero. Measurements were considered outliers and excluded for further analysis when they fell outside the interquartile range (i.e., between $Q1 - 1.5 \times \text{IQR}$ and $Q3 + 1.5 \times \text{IQR}$, where $Q1$ is the first quartile, $Q3$ is the third quartile, and IQR is the difference between $Q1$ and $Q3$, Lin et al., 2020). At each site in each season, at least 10 random and non-repeating replicates of CO₂ flux measurements were obtained.

At each site for each measurement, the chambers were exposed *in situ* to a series of five different irradiances (0, 30, 50, 70, and 100% shading) by covering the chambers with screens with different meshes or an opaque fabric to determine the CO₂ flux as a function of the incident irradiance (i.e., P-I curve) on the sediment. This P-I curve can be described by the equation of Jassby and Platt (1976):

$$\text{GPP} = \text{GPP}_m \tanh(\alpha E / \text{GPP}_m) \quad (2)$$

where GPP_m is the maximum GPP (in $\text{mg C m}^{-2} \text{ h}^{-1}$) in the absence of photoinhibition under optimal irradiance, α is the initial slope of the P-I curve, and E is the irradiance measured as PAR (in $\mu\text{mol quanta m}^{-2} \text{ s}^{-1}$). P-I curves were drawn in Sigmaplot (version 12.5; Systat Software Inc., San Jose, CA, United States) for non-linear regression fitting, and the results were acceptable when the fit was significant ($p < 0.05$) and the determination coefficient was larger than 0.80 (Supplementary Figure 1).

Environmental and Biological Variables

After each CO₂ flux measurement, the top 5 cm of the sediment inside each chamber was sampled by a cutoff syringe with a 2.6 cm inner diameter for sediment characterization and interstitial nutrient analyses. The sediment grain size, sorting coefficient, and mud content were determined by the standard wet-sieved method (Bale and Kenny, 2005) and the modified pipette method (Hsieh and Chang, 1991). Fine materials, such

as clay and silt, referred to as mud (grain size < 63 μm). The sediment organic matter content was measured by the loss-on-ignition method (Bale and Kenny, 2005). Sediment interstitial water from the top 5 cm layer was collected, filtered through Whatman GF/C glass fiber filters, stored at 4°C, and then brought to the laboratory for nutrient analysis. A spectrophotometer (U-5100, Hitachi, Tokyo, Japan) was used for the determination of nitrite (Bendschneider and Robinson, 1952), nitrate (Jenkins and Medsker, 1964), ammonia (Pai et al., 2001), and phosphate (Murphy and Riley, 1962). The salinity of the interstitial water was measured by a portable conductivity meter (ProfiLine Cond 3310, WTW, Weilheim, Germany).

After each CO₂ flux measurement, the biomasses of benthic microalgae and macrofauna inside the chamber were also determined. The top 1 cm of the sediment, where most benthic microalgae are located (Cadée and Hegeman, 1974), was sampled by a cutoff syringe with a 1 cm inner diameter (six replicates for each chamber). The sediment samples were then frozen until they were brought to the laboratory. The chlorophyll *a*, *b*, and *c* concentrations were measured by the acetone method (Jeffrey and Humphrey, 1975). While the chlorophyll *a* concentration can be a proxy for the total biomass of benthic microalgae, the chlorophyll *b* and *c* concentrations indicate the biomass of green algae and diatoms in tidal flats, respectively (Golterman, 1975). For collecting macrofauna, the top 10 cm of the sediment was sampled by a stainless steel ring corer with a 10 cm inner diameter (one sample for each chamber). The sediment samples were then strained with a 0.5 mm sieve and preserved in 70% ethanol in the field. After being brought back to the laboratory, the macrofauna samples were sorted, counted and weighed by oven-drying (60°C) to a constant weight and then combusted at 500°C for 4 h to determine the ash-free dry weight (AFDW).

Data Analysis

Since our data failed in the normality test and did not meet the assumptions for a one-way ANOVA, the Kruskal–Wallis test was used to examine whether the sediment characteristics differed among the nine study sites. When significant differences ($p < 0.05$) were detected, Dunn's multiple comparisons test was further used to determine which means differed.

Structural equation models (SEM) were used to assess the hypothesized direct and indirect effects of sediment characteristics and the biomasses of benthic microalgae and macrofauna on the primary production and respiration of the tidal flats. To answer such fundamental questions, we needed a mechanistic understanding of the relationships among the potential factors and their relative importance. By testing multivariate hypotheses and considering the direct and indirect effects of multiple interacting variables, SEM is a multivariate technique suitable to test networks of causal models (Eisenhauer et al., 2015).

Since sediment mud content is closely related to other sediment characteristics, such as grain size, organic matter content, sorting coefficient and interstitial nutrient content, sediment mud content was used as the proxy for the sediment characteristics in the conceptual SEM (Figure 2).

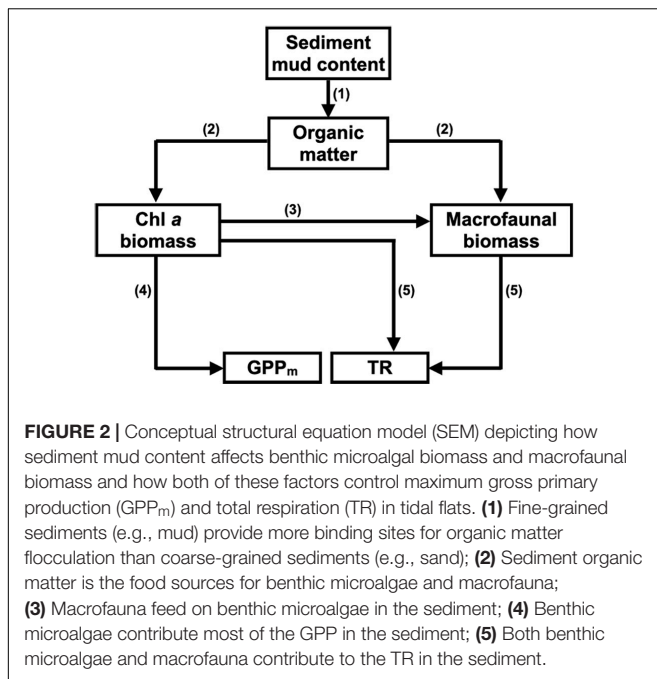
TABLE 2 | Sediment characteristics of the tidal flats.

Site		Sediment temperature (°C)		Sediment salinity	Sediment organic matter content (%)	Sediment grain size (μm)	Sediment mud content (%)	Sediment sorting coefficient	Benthic chl a concentration (mg m ⁻²)	Macrofaunal biomass (g AFDW m ⁻²)	Interstitial DIN concentration (μM)	Interstitial DIP concentration (μM)
		Winter	Summer									
#1	Siangshan (SS; n = 44)	17.5 ~ 34.7	33.1 ~ 38.5	15.0 ~ 45.5	0.5 ~ 1.6	54.9 ~ 208.2	7.7 ~ 48.2	0.50 ~ 1.26	44.6 ~ 163.3	0.00 ~ 62.35	5.6 ~ 322.2	0.50 ~ 8.80
		26.2 ± 5.8	36.0 ± 2.0	32.3 ± 5.3 ^{ab}	0.9 ± 0.3 ^{cd}	112.2 ± 37.2 ^{de} (very fine sand)	21.5 ± 10.6 ^{cd}	1.04 ± 0.16 ^b	84.7 ± 29.9 ^{bc}	6.19 ± 13.23 ^{ac}	138.1 ± 75.3 ^c	2.45 ± 1.48 ^b
#2	Houlong (HL; n = 31)	15.3 ~ 22.2	29.8 ~ 34.7	17.8 ~ 37.2	0.9 ~ 2.7	28.7 ~ 341.5	0.1 ~ 64.1	0.46 ~ 2.06	1.0 ~ 118.1	0.0076.83	15.8 ~ 375.7	0.07 ~ 3.17
		18.7 ± 2.7	32.5 ± 1.6	30.5 ± 4.4 ^{ab}	1.6 ± 0.6 ^{ab}	190.2 ± 89.3 ^{bcd} (fine sand)	11.4 ± 18.0 ^{cd}	0.97 ± 0.49 ^{bc}	22.7 ± 27.0 ^e	0.95 ± 1.92 ^{de}	124.0 ± 110.9 ^{cd}	1.60 ± 0.68 ^{bc}
#3	Fangyuan (FY; n = 24)	19.0 ~ 29.2	34.5 ~ 36.4	13.1 ~ 35.3	1.5 ~ 2.7	35.6 ~ 101.1	30.6 ~ 87.6	0.82 ~ 1.49	23.8 ~ 97.0	0.00 ~ 112.81	112.0 ~ 433.4	1.85 ~ 66.54
		23.1 ± 3.7	35.3 ± 0.6	25.1 ± 7.0 ^b	2.0 ± 0.3 ^a	57.7 ± 21.0 ^f (silt)	66.7 ± 17.7 ^{ab}	1.18 ± 0.19 ^b	52.8 ± 17.2 ^{cde}	16.93 ± 33.03 ^a	239.1 ± 110.6 ^{ac}	11.06 ± 14.98 ^a
#4	Haomeiliao (HML; n = 20)	22.8 ~ 29.0	34.8 ~ 40.9	30.8 ~ 36.0	0.8 ~ 2.1	39.3 ~ 133.0	2.8 ~ 73.6	0.43 ~ 1.22	5.1 ~ 72.5	0.00 ~ 66.90	50.4 ~ 217.0	0.52 ~ 1.02
		25.7 ± 2.8	36.3 ± 1.7	33.9 ± 1.3 ^a	1.2 ± 0.4 ^{bc}	81.2 ± 29.8 ^{ef} (very fine sand)	33.3 ± 21.3 ^{bc}	0.93 ± 0.21 ^b	29.8 ± 20.0 ^{de}	14.40 ± 20.44 ^a	149.5 ± 78.0 ^{bode}	0.83 ± 0.20 ^{bcd}
#5	Gaoping (GP; n = 39)	21.9 ~ 31.5	27.6 ~ 35.9	2.1 ~ 30.1	0.8 ~ 2.3	10.2 ~ 339.2	2.7 ~ 99.9	0.60 ~ 1.76	1.0 ~ 244.0	0 ~ 6.19	2.0 ~ 3942.4	0.05 ~ 3.63
		27.6 ± 3.2	33.1 ± 2.6	14.5 ± 8.0 ^c	1.5 ± 0.3 ^{ab}	59.0 ± 68.6 ^f (silt)	76.9 ± 24.3 ^a	1.11 ± 0.34 ^b	70.7 ± 58.3 ^{bcd}	0.88 ± 1.46 ^{bcd}	512.0 ± 969.4 ^c	0.84 ± 0.66 ^d
#6	Nangan (NG; n = 24)	13.4 ~ 18.8	27.8 ~ 34.4	12.5 ~ 41.4	0.6 ~ 3.4	126.2 ~ 567.8	0.6 ~ 27.9	0.77 ~ 2.23	35.9 ~ 219.3	0 ~ 76.41	171.1 ~ 21915.9	0.51 ~ 36.54
		16.0 ± 1.6	31.2 ± 2.3	30.0 ± 5.1 ^b	1.4 ± 0.7 ^{bc}	258.7 ± 96.9 ^{abc} (medium sand)	9.7 ± 8.1 ^{de}	1.53 ± 0.42 ^a	107.9 ± 43.1 ^{ab}	14.07 ± 20.64 ^a	4789.6 ± 6084.1 ^{ab}	5.31 ± 9.45 ^b
#7	Beishan (BS; n = 34)	16.2 ~ 34.2	34.7 ~ 47.4	30.0 ~ 35.3	0.5 ~ 3.2	55.3 ~ 395.9	9.7 ~ 57.2	1.69 ~ 3.08	77.2 ~ 385.6	0 ~ 44.87	11.1 ~ 157.4	0.29 ~ 10.42
		22.7 ± 5.9	40.6 ± 3.6	32.6 ± 1.8 ^{ab}	1.6 ± 0.6 ^{ab}	166.7 ± 99.4 ^{cd} (fine sand)	29.4 ± 12.0 ^c	2.05 ± 0.30 ^a	146.8 ± 66.4 ^a	8.96 ± 12.63 ^a	49.7 ± 37.6 ^{df}	3.59 ± 2.79 ^{abc}
#8	Wujiang (WJ; n = 25)	16.7 ~ 26.3	34.7 ~ 46.9	25.0 ~ 35.0	0.2 ~ 2.0	323.8 ~ 720.3	0.0 ~ 3.5	0.79 ~ 1.44	80.2 ~ 380.3	0 ~ 3.76	27.2 ~ 550.7	0.18 ~ 23.17
		22.2 ± 3.4	40.5 ± 4.3	31.0 ± 2.2 ^{ab}	0.5 ± 0.5 ^{de}	552.1 ± 97.1 ^a (coarse sand)	1.0 ± 1.0 ^{ef}	1.02 ± 0.15 ^b	177.5 ± 80.4 ^a	0.90 ± 0.99 ^c	127.0 ± 135.6 ^{cdf}	4.19 ± 5.08 ^{ab}
#9	Oucuo (OC; n = 22)	12.0 ~ 26.3	32.2 ~ 46.7	15.6 ~ 35.0	0.2 ~ 0.4	207.8 ~ 678.3	0.0 ~ 0.3	0.33 ~ 0.99	7.2 ~ 42.2	0 ~ 26.54	4.8 ~ 47.4	0.37 ~ 3.71
		23.1 ± 5.4	39.1 ± 4.9	29.2 ± 4.0 ^b	0.3 ± 0.1 ^e	319.6 ± 122.4 ^{ab} (medium sand)	0.09 ± 0.07 ^f	0.66 ± 0.23 ^c	20.6 ± 10.5 ^e	2.44 ± 6.10 ^{ce}	22.9 ± 13.0 ^{ef}	1.52 ± 0.86 ^{bcd}

Data are presented as the range and mean ± SD.

For each variable, different letters after the data (mean ± SD) indicate significant differences among sites.

chl a, chlorophyll a; AFDW, ash-free dry weight; DIN, dissolved inorganic nitrogen (NO₂ + NO₃ + NH₄); DIP, dissolved inorganic phosphorus (PO₄).



Since sediment characteristics can also affect the composition of benthic microalgae, an alternative conceptual SEM was constructed to assess the potential effects of benthic microalgal composition on the CO₂ fluxes in the tidal flats. We used a composite variable that represented a combination of the chlorophyll *a*, *b*, and *c* concentrations to replace the chlorophyll *a* concentration (the total biomass of benthic microalgae) only for SEM analysis. The composite variable originated from the total combined influence of the measured variables (Grace and Bollen, 2008) and was the sum of all variables involved, depending on the different weights the variables were expected to have. The weights of each variable were derived from the coefficients of the multiple regression of GPP_m with the chlorophyll *a*, *b*, and *c* concentrations of benthic microalgae.

Piecewise SEM was used to test the validity of the conceptual models (Lefcheck, 2016); this approach allowed the fitting of generalized linear mixed models with a hierarchical design (Figure 2). We used Shipley's test of direct separation (*d*-test) to assess the overall fit of the models. The model was acceptable when the *p*-value of the chi-square test of Fisher's *C* statistic was higher than the significance level ($p > 0.05$). Fisher's *C* test was related to all the unspecified paths of the conceptual models. When one or more of these unspecified paths presented significant importance, the model did not have a good fit, as the *p*-value of the chi-square test of Fisher's *C* statistic was lower than 0.05. Therefore, these missing paths included required information and needed to be added to the conceptual model. We fitted our conceptual model as a generalized linear model with a Tweedie distribution (Tweedie, 1984) because our data were distributed from zero to positive values. The piecewise SEM was performed by using the 'psem' function from the R package 'piecewiseSEM' (Lefcheck, 2016). The standardized path coefficients were determined using the bootstrap method from

the R package 'semEff' (Murphy, 2020). All above statistical analyses were performed with the statistical software R version 4.0.4 (R Core Team, 2021).

RESULTS

Sediment Granulometry

Based on the grain size data, the sediments at the nine tidal flats were classified into five categories: coarse sand (#8 WJ), medium sand (#6 NG, #9 OC), fine sand (#2 HL, #7 BS), very fine sand (#1 SS, #4 HML) and silt (#3 FY, #5 GP) sediment. The median grain size averaged between 57.7 and 552.1 μm, and the mud content averaged from 0.1 to 76.9% (Table 2). The increases in sediment mud content were also concomitant with changes in the sorting coefficient and the interstitial dissolved inorganic nitrogen (DIN) concentration (Table 3).

Benthic Microalgal and Macrofaunal Biomass

The benthic chlorophyll *a* concentration ranged from 12.5 to 221.3 mg m⁻², with an average concentration of 78.8 mg m⁻² for all the samples analyzed (Figure 3A). Of the sites, #8 WJ in summer (221.3 ± 96.2 mg m⁻²) and #7 BS in winter (168.8 ± 77.4 mg m⁻²) had the highest observed benthic chlorophyll *a* concentrations. The lowest values of the benthic chlorophyll *a* concentration were observed at #9 OC in both summer and winter (28.8 ± 8.9 mg m⁻², 12.5 ± 2.9 mg m⁻²).

The macrofauna in the top 10 cm of the sediment of the tidal flats were mainly bivalves, decapods, gastropods, amphipods, and polychetes (Supplementary Table 1). The macrofaunal biomass in terms of ash-free dry weight (g AFDW m⁻²) varied among the nine study sites, ranging from 0.1 to 28.6 g AFDW m⁻². The macrofaunal biomass showed the highest values at #4 HML (27.7 ± 22.0 g AFDW m⁻²) in summer and at #6 NG (20.4 ± 27.0 g AFDW m⁻²) in winter but the lowest values at #5 GP (0.1 ± 0.3 g AFDW m⁻²) in summer and at #9 OC (0.5 ± 0.5 g AFDW m⁻²) in winter (Figure 3B). The macrofaunal density also varied among the nine study sites, ranging from 0.01 to 0.63 ind. m⁻². The highest values of macrofaunal density appeared at #7 BS (0.34 ± 0.40 ind. m⁻²) in summer and at #1 SS (0.48 ± 0.41 ind. m⁻²) in winter, while the lowest values appeared at #2 HL (0.01 ± 0.02, 0.01 ± 0.01 ind. m⁻²) in both summer and winter (Figure 3C).

Benthic Carbon Dioxide Fluxes

During emersion, GPP_m showed a clear seasonal pattern with higher values in winter and lower values in summer at most of the study sites except for #8 WJ and #9 OC (Figure 4A). Of the sites, #5 GP had the highest values of GPP_m in both summer and winter (76.5 ± 21.2 and 89.7 ± 41.7 mg C m⁻² h⁻¹, respectively). The lowest values of GPP_m were observed at #3 FY in summer (1.2 ± 1.1 mg C m⁻² h⁻¹) and at #9 OC in winter (4.4 ± 3.5 mg C m⁻² h⁻¹). GPP_m was positively correlated with benthic chlorophyll *a* concentration, sorting coefficient and mud content but negatively correlated with interstitial dissolved inorganic phosphorus (DIP) concentration (Table 3).

TABLE 3 | Spearman rank correlation coefficients between (A) environmental variables and (B) environmental variables and carbon fluxes in the tidal flats.

	Temp	Light	Chl <i>a</i>	AFDW	Density	Sorting	Mud	DIN	DIP
(A) Environmental variable									
Light	0.08								
Chl <i>a</i>	0.08	-0.16*							
AFDW	0.12	-0.13*	0.28***						
Density	0.05	-0.09	0.45***	0.62***					
Sorting	-0.02	-0.03	0.45***	0.20**	0.13*				
Mud	0.02	0.01	0.01	-0.02	-0.01	0.32***			
DIN	0.00	-0.25***	0.25***	0.15*	0.13	0.14	0.19*		
DIP	0.09	0.05	0.19**	0.06	-0.01	0.16*	-0.08	0.10	
(B) Carbon flux									
GPP _m	0.00	-0.02	0.24***	-0.11	0.06	0.21**	0.32***	-0.09	-0.26***
TR	0.36	-0.05	0.22***	0.10	0.19**	0.29***	0.56***	0.29***	-0.01
NPP	-0.10	0.05	0.14*	-0.19**	-0.03	0.18**	0.29***	-0.14*	-0.32***

Temp, sediment temperature; Light, irradiance; Chl *a*, benthic chlorophyll *a* concentration; AFDW, macrofaunal biomass in terms of ash-free dry weight; Density, macrofaunal density; Sorting, sediment sorting coefficient; Mud, sediment mud content; DIN, interstitial dissolved inorganic nitrogen (NO₂ + NO₃ + NH₄) concentration; DIP, interstitial dissolved inorganic phosphorus (PO₄) concentration; GPP_m, maximum gross primary production; TR, total respiration; NPP, net primary production. **p* < 0.05, ***p* < 0.01, ****p* < 0.001.

Total respiration (TR) had an opposite seasonal pattern to that of GPP_m at most of the study sites, with higher values in summer and lower values in winter except at #5 GP (Figure 4B). The highest values of TR occurred at #6 NG in summer (17.5 ± 14.2 mg C m⁻² h⁻¹) and at #5 GP in winter (15.3 ± 7.5 mg C m⁻² h⁻¹). The lowest values of TR occurred at #8 WJ in summer (1.5 ± 0.4 mg C m⁻² h⁻¹) and #2 HL in winter (1.0 ± 0.4 mg C m⁻² h⁻¹). TR was positively correlated with benthic chlorophyll *a* concentration, sorting coefficient, mud content, and interstitial DIN concentration (Table 3).

The seasonal pattern of NPP was similar to that of GPP_m (Figure 4C). The highest values of NPP appeared at #5 GP in both summer and winter (59.1 ± 26.2 and 68.1 ± 37.0 mg C m⁻² h⁻¹, respectively). The lowest values of NPP appeared at #3 FY in summer (-17.9 ± 6.4 mg C m⁻² h⁻¹) and at #9 OC in winter (1.8 ± 3.2 mg C m⁻² h⁻¹). Notably, the NPP values for the tidal flats at #1 SS, #3 FY, and #6 NG during emersion shifted to negative values in summer, indicating that these sites functioned as carbon sources. The NPP values were positively correlated with benthic chlorophyll *a* concentration, macrofaunal biomass, sorting coefficient and mud content but negatively correlated with interstitial DIN and DIP concentrations.

All values of GPP_m, TR and NPP for the tidal flats during emersion increased significantly with increasing sediment mud content (Figure 5). Significant linear increases in GPP_m ($y = 0.586x + 5.574$, $r^2 = 0.386$, $p < 0.01$) and NPP ($y = 0.398x + 3.201$, $r^2 = 0.251$, $p = 0.034$) were apparent when the sediment mud content ranged from 0 to 90%. However, there was high variability in the muddier sediments (Figures 5A,C). The TR ($y = 0.126x + 2.212$, $r^2 = 0.400$, $p < 0.01$) curve was similar to the curves of GPP_m and NPP (Figure 5B).

SEM Models

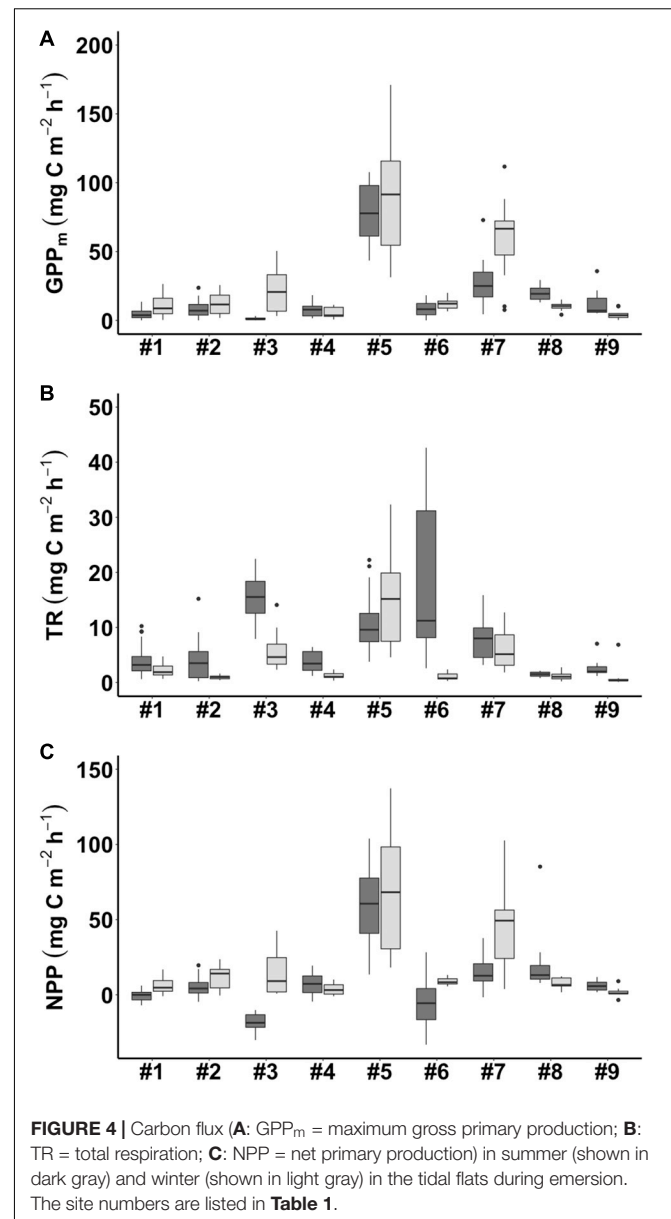
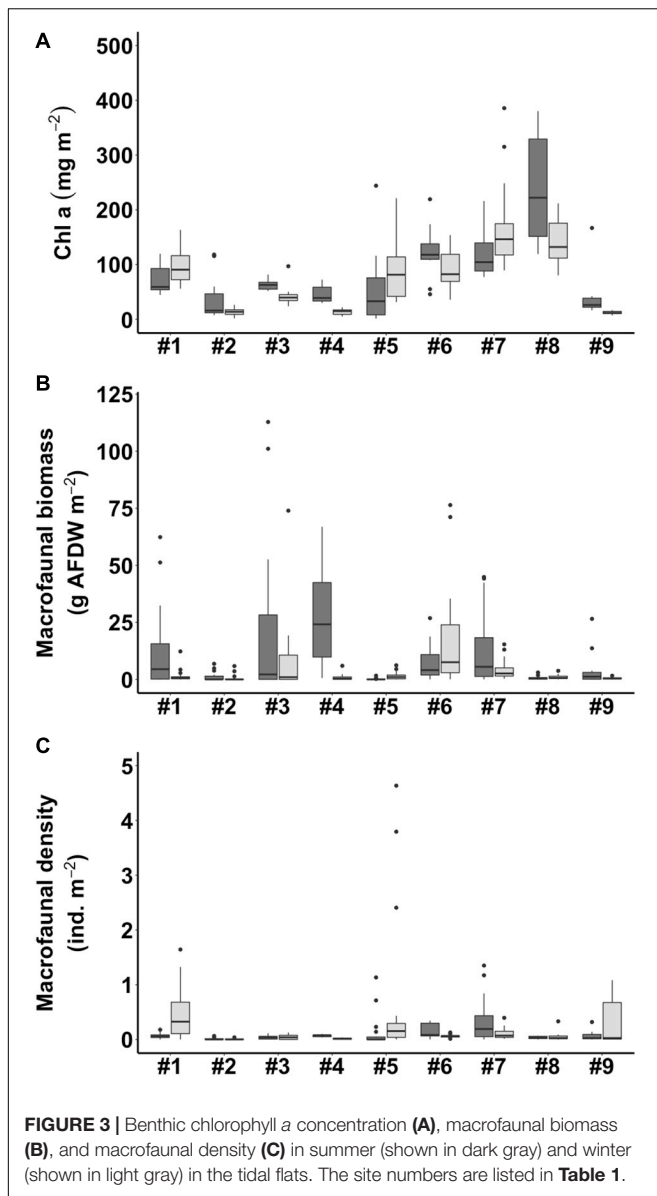
Based on the resulting correlations (Table 3), the piecewise SEM fit the observed data well (Fisher's *C* statistic = 8.95, $p = 0.062$) and revealed that the sediment mud content affected

primary production and respiration in tidal flats both directly and indirectly (Figure 6A). The sediment mud content directly increased the organic matter content [0.436, 95% confidence interval (CI): 0.356–0.504, $p < 0.001$]. The sediment mud content also directly increased GPP_m (0.233, 95% CI: 0.154–0.368, $p < 0.001$) but had an indirect, weak and negative effect on GPP_m via benthic microalgal biomass (-0.180 × 0.117). The sediment mud content also showed a direct and positive effect on TR (0.273, 95% CI: 0.119–0.389, $p < 0.001$) and indirectly increased TR (0.436 × 0.175) via the organic matter content. Benthic microalgal biomass showed a direct and positive effect on TR. However, there was no direct or indirect effect on TR via benthic macrofaunal biomass.

The alternative SEM replaced with microalgal composition (Figure 6B) also fit the observed data well (Fisher's *C* = 15.52, $p = 0.114$). The pathways by which sediment mud content influenced TR remained unchanged. In addition to a direct effect on GPP_m (0.208, 95% CI: 0.124–0.347, $p < 0.001$), the sediment mud content showed an indirect effect on GPP_m (0.381 × 0.053) via a compositional shift in benthic microalgae.

DISCUSSION

Despite the spatial variation in the sediment characteristics, the CO₂ fluxes in the tidal flats during emersion in the tropical and subtropical regions increased with increasing sediment mud content. Our results showed clear positive linear gradients in GPP_m, TR, and NPP from sandy to muddy sediments (Figure 5). The SEM further revealed the possible causal pathways by which sediment mud content directly increased GPP_m or indirectly increased GPP_m via a benthic microalgal compositional shift (Figure 6). The SEM also revealed that sediment mud content directly increased TR or indirectly increased TR via organic matter content (Figure 6). With the integrated SEM framework, our results showed mechanistic evidence of how sediment

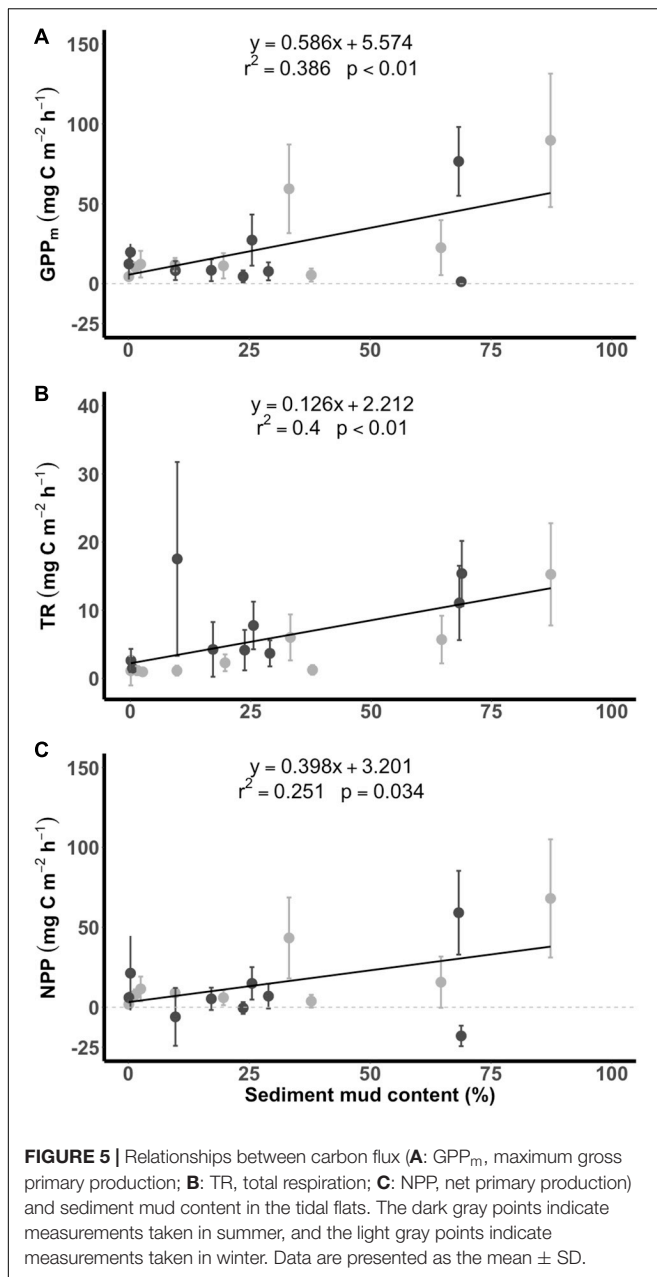


mud content acted as a critical factor regulating carbon fluxes in tidal flats.

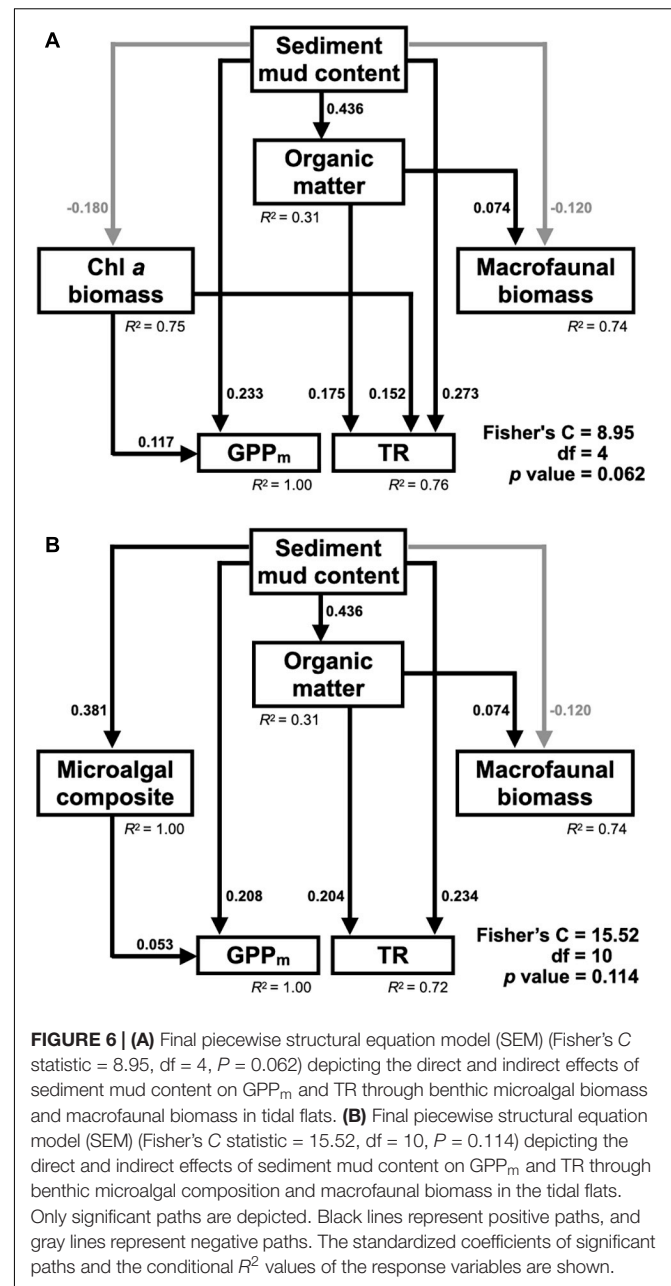
Despite the critical role of sediment mud content in regulating carbon fluxes, prior studies showed inconsistent relationships between benthic chlorophyll *a* concentration and sediment mud content. Both Cahoon et al. (1999) and Cahoon and Safi (2002) reported negative relationships between the proportion of very fine sediments and benthic microalgal biomass in tidal flats in the US and on the North Island of New Zealand. However, both Lee et al. (2011) and Pratt et al. (2015) showed an opposite trend, i.e., that benthic microalgal biomass was positively correlated with sediment mud content. In this study, there was no significant correlation between the benthic chlorophyll *a* concentration and sediment mud content. In fact, the benthic chlorophyll *a* concentration was higher in the sandy sediments at the NG, BS, and WJ sites than at the other sites; in addition, the sediments

of these three sites were categorized as medium, fine and coarse sand, respectively. The median grain size at these sampling sites ranged from 166.7 to 552.1 μm , and all the mud content values were lower than 30%. The SEM showed that in comparison to the muddy sediments, the sandy sediments supported more microalgal biomass in the tidal flats.

The greater microalgal biomass in the sandy sediments than in the muddy sediments can be attributed to the thicker photic zone in the sandy sediments. The photic zone in muddy sediments is shallow (<600 μm ; Cartaxana et al., 2011, 2006), and benthic microalgae are required to move up and down with diurnal and tidal cycles to maintain photosynthesis. In comparison to algal cells at deeper depths, algal cells that must remain near the sediment surface might be more susceptible to resuspension by tides and waves and



epifaunal grazing. However, the photic depth can extend to 3 mm in sandy sediments (Cartaxana et al., 2006, 2011). Since light can penetrate deeper into coarse sediments, benthic microalgae can be distributed more evenly throughout the thicker photic layer. The other possibility for this outcome is that the composition of benthic microalgae in the muddy sediments was different from that in the sandy sediments (Du et al., 2009). In muddy sediments, the benthic microalgal community is generally dominated by epipellic benthic diatoms that exhibit endogenous vertical migratory rhythms coupled with diurnal and tidal cycles (Consalvey et al., 2004; Haubois et al., 2005). They often aggregate as a dense and highly productive biofilm at the surface of sediment during low tide



in the daytime (Cartaxana et al., 2011). In sandy sediments, the benthic microalgae community composition is generally dominated by epipsammic benthic diatoms that attach to sand particles across the deeper photic layer and do not exhibit migratory patterns (Consalvey et al., 2004). The algal cells near the sediment surface might also be more susceptible than algal cells at deeper depths to grazing by macrofauna. Other factors, such as interstitial space volume, grazing pressure, nutrient fluxes, and light penetration, may confound the relationship between benthic microalgal biomass and sediment granulometry; any combination of these factors might lead to lower or higher benthic microalgal biomass in tidal flats, which might mask the relationship with sediment mud content.

Hydrodynamics might also affect the response of benthic microalgal biomass to sandy sediments. Dalu et al. (2020) conducted a microcosm experiment and found that the benthic chlorophyll *a* concentration was the highest in sediments with coarser particle sizes ranging from 125 to 500 μm , which was comparable to our results. However, the sediment grain sizes at #2 HL and #9 OC both fell into this range, but the chlorophyll *a* concentration at these sites was low (Table 2). Compared with those at the #6 NG and #7 BS sites, significantly lower sediment sorting coefficients at #2 HL and #9 OC were also observed. The sediment sorting coefficient was used to assess the distribution of the grain sizes in sediments. Well-sorted sediment indicates that the distribution of grain sizes is even; these sediments might be fully winnowed by waves and tidal currents. Contrary to muddy sediment, where benthic microalgae normally form dense biofilms embedded within a matrix comprised of carbon exudates (commonly known as EPS) that protect them from erosion, such high-energy forces can resuspend or remove not only small particles but also benthic microalgal cells inhabiting the sandy sediment.

Sediment mud content can also influence the density of macrofauna in tidal flats. Pratt et al. (2014) studied nine estuaries on the North Island of New Zealand and found that the densities of a suspension feeder (*Austrovenus stutchburyi*) and a deposit feeder (*Macomona liliana*) decreased significantly with increasing sediment mud content, although the gradient of the mud content ranged only between 0 and 30%. Other studies have indicated that the effects of sediment mud content on macrofaunal abundance were species-dependent (Thrush et al., 2003; Ellis et al., 2006; Anderson, 2008). For example, the relationships between the density of polychetes and sediment mud content can be classified into three types: an increasing curve (*Scolecopides benhami*), a decreasing curve (*Aonides oxycephala*) and a Gaussian response curve (*Heteromastus filiformis*; Thrush et al., 2003). In this study, benthic macrofaunal biomass was high either in muddy sediments (FY and HML) or in sandy sediments (NG) and did not show a significant correlation with sediment mud content (Table 3). The macrofaunal community mainly contained bivalves, decapods, gastropods, amphipods, and polychetes, which might have masked the individual response of each taxon to the sediment mud content. However, the SEM showed that in total, in comparison to the muddy sediments, the sandy sediments supported more macrofaunal biomass in the tidal flats.

The primary production (GPP_m and NPP) was higher in winter than in summer at most of the studied sites except at #8 WJ and #9 OC, while the total respiration (TR) in the tidal flats was higher in summer than in winter at most of the studied sites except at #5 GP. Temperature has been reported to be a major driver of the seasonal variation in the CO_2 fluxes in subtropical tidal flats (Lee et al., 2011). Higher temperatures generally stimulate metabolic processes and photosynthesis rates. Lin et al. (2020) further indicated that the effects of temperature on the CO_2 fluxes in tidal flats were non-linear, showing a quadratic relationship with an optimal temperature at which the CO_2 fluxes were highest. In this study, the sediment temperatures in summer ranged from 31.2°C to 40.6°C, which far exceeded

the optimal temperatures (28.7°C for GPP_m , 26.6°C for NPP; Lin et al., 2020) for primary production. Higher temperatures might also result in photoinhibition in benthic microalgae (Laviale et al., 2015). These temperatures can explain the decreases in GPP_m and NPP in summer. In contrast, the sediment temperature in winter ranged from 16.0°C to 27.6°C, which was within the range of optimal temperatures (45°C; Lin et al., 2020) for benthic respiration in tidal flats. This scenario might be the reason that the TR in the tidal flats still increased in summer at most of the study sites.

Hydrodynamics may affect the primary production and respiration in tidal flats during immersion in different ways. Wind- or tide-induced disturbances may increase water turbidity in tidal flats. Increased water turbidity can decrease light availability on the sediment and then reduce the photosynthesis of benthic microalgae (Migné et al., 2009). Drylie et al. (2018) measured GPP in three unvegetated sandflats in Kaipara Harbour, New Zealand and found that the submerged GPP was significantly lower than the emerged GPP due to light limitation. However, respiration was generally higher under immersed condition than under emerged condition due to the elevated activity of infauna during inundation (Migné et al., 2009). Lee et al. (2011) further demonstrated that turbid water increased respiration during immersion in subtropical tidal flats. It is clear that the CO_2 fluxes in tidal flats located in the shallow waters along the coast of marginal seas are prone to disturbances caused by wind or tide.

In the SEM, the direct effect of the sediment mud content on GPP_m was stronger than the indirect effect via benthic chlorophyll *a* content. This result suggests that in comparison to microalgal biomass, the sediment mud content had a more direct influence on GPP_m . Compared to those in sandy sediments, the reduced interstitial volumes in muddy sediments might have allowed more water retention among grain particles (Watermann et al., 1999; Lee et al., 2011), which might have resulted in the accumulation of regenerated nutrients and organic matter that stimulated the growth of benthic microalgae in the sediments (Ehrenhauss et al., 2004). However, in the alternative SEM replaced with the composition of benthic microalgae, there was a weak and indirect effect of sediment mud content on GPP_m via the composition shift of benthic microalgae. In this study, the chlorophyll *c* concentration as a proxy of diatom biomass in the tidal flats decreased with increasing sediment mud content ($y = -0.188x + 12.478$, $r^2 = 0.189$, $p < 0.001$), whereas the chlorophyll *b* concentration as a proxy of green algal biomass remained unchanged. Sediment granulometry has been reported to shift the composition of the benthic microalgal community in tidal flats (Underwood and Barnett, 2006). Some epipelagic diatoms with large and long valves occur in finer sediments, whereas small species of diatoms inhabit coarser sediments (Du et al., 2009). In western Taiwan, Shiu (2009) found that the density of benthic diatoms with larger biovolumes was negatively correlated with sediment grain size. Although the biomass of diatoms decreased in muddy sediments, the diatom community may have shifted to diatoms with large biovolumes. Since diatoms with large biovolumes generally have higher photosynthetic rates

(Taguchi, 1976; Geider et al., 1986), the GPP_m is expected to increase with increasing mud content in the sediments.

The SEM showed a significant indirect effect of sediment mud content on TR via organic matter content. However, the contribution of benthic microalgal and macrofaunal biomass to TR was relatively minor. This result is not surprising because in comparison to macrofauna and meiofauna, the bacterial community in tidal flats generally plays a more vital role in benthic respiration and contributes much more to the total respiration (Piepenburg et al., 1995; Hubas et al., 2006). Bacterial respiration can account for 67–88% of the annual benthic respiration in shallow waters (Piepenburg et al., 1995; Hubas et al., 2007). Moreover, the dynamics of bacterial communities are strongly regulated by granulometry (Hubas et al., 2006). Our results further suggest that the sediment mud content influenced the TR in the tidal flats not by increasing the biomasses of benthic microalgae and macrofauna but by influencing the metabolism of the bacterial community.

CONCLUSION

In the nine studied tidal flats in tropical and subtropical regions during emersion at noon, GPP_m and NPP had higher values in winter than in summer due to the sediment temperature in summer deviating from the optimal temperature. In contrast, TR had higher values in summer than in winter because the sediment temperature in summer was still within the optimal temperature range. All the values of GPP_m , TR, and NPP increased significantly with increasing sediment mud content. The SEM further showed mechanistic evidence of how sediment mud content can be a critical factor regulating carbon fluxes in tidal flats. The sediment mud content directly increased GPP_m or indirectly increased GPP_m via a compositional shift in benthic microalgae. The sediment mud content also directly increased TR or indirectly increased TR via increased organic matter content. Considering the large proportion of unvegetated tidal flats in coastal zones, any anthropogenic activity or natural forcing that eventually leads to a change in sediment mud content will likely substantially change the carbon sequestration capacity in those coastal ecosystems.

REFERENCES

- Anderson, M. J. (2008). Animal-sediment relationships re-visited: characterising species' distributions along an environmental gradient using canonical analysis and quantile regression splines. *J. Exp. Mar. Biol. Ecol.* 366, 16–27. doi: 10.1016/j.jembe.2008.07.006
- Bale, A. J., and Kenny, A. J. (2005). "Sediment analysis and seabed characterisation," in *Methods for the Study of Marine Benthos*, eds A. Eleftheriou and A. McIntyre (Hoboken, NJ: Blackwell Science Ltd), 43–86. doi: 10.1002/9780470995129.ch2
- Bendschneider, K., and Robinson, R. J. (1952). A new spectrophotometric method for the determination of nitrite in sea water. *J. Mar. Res.* 11, 87–96.
- Billerbeck, M., Røy, H., Bosselmann, K., and Huettel, M. (2007). Benthic photosynthesis in submerged Wadden Sea intertidal flats. *Estuar. Coast. Shelf Sci.* 71, 704–716. doi: 10.1016/j.ecss.2006.09.019
- Brotas, V., and Catarino, F. (1995). Microphytobenthos primary production of Tagus estuary intertidal flats (Portugal). *Netherlands J. Aquat. Ecol.* 29, 333–339. doi: 10.1007/BF02084232

DATA AVAILABILITY STATEMENT

The original contributions presented in the study are included in the article/**Supplementary Material**, further inquiries can be directed to the corresponding author/s.

AUTHOR CONTRIBUTIONS

W-JL and H-JL conceived the ideas and designed the study. W-JL carried out the field work and sampling quantification. W-JL, C-WL, M-CC, and H-JL contributed to the data analysis and interpretation. W-JL and H-JL drafted the manuscript. All authors read and approved the final manuscript.

FUNDING

This work was funded by (1) Kinmen National Park Headquarters, Ministry of Interior, Taiwan and (2) the "Innovation and Development Center of Sustainable Agriculture" project administered by the "Featured Areas Research Center program" within the framework of Taiwanese Ministry of Education's "Higher Education Sprout Project."

SUPPLEMENTARY MATERIAL

The Supplementary Material for this article can be found online at: <https://www.frontiersin.org/articles/10.3389/fmars.2021.670180/full#supplementary-material>

Supplementary Figure 1 | Photosynthesis-irradiance (P-I) curves during emersion in summer and winter in the tidal flats. Different symbols represent different samplings in each season at each site. P-I curves with determination coefficients larger than 0.80 are shown. No P-I curve at FY in summer is shown because the GPP values under different light irradiances were zero.

Supplementary Table 1 | Density of each group of macrofauna in the tidal flats. Data are presented as the range and mean \pm SD. Zero represents no occurrence of each taxon in the tidal flats. Only samplings with macrofauna were averaged.

Supplementary Table 2 | CO_2 fluxes (in $mg\ C\ m^{-2}\ h^{-1}$) measured in the tidal flats. Data are presented as the range, mean \pm SD and 95% confidence interval.

- Cadée, G. C., and Hegeman, J. (1974). Primary production of the benthic microflora living on tidal flats in the dutch wadden sea. *Netherlands J. Sea Res.* 8, 260–291. doi: 10.1016/0077-7579(74)90020-9
- Cahoon, L. (1999). The role of benthic microalgae in neritic ecosystems. *Oceanogr. Mar. Biol. an Annu. Rev.* 37, 47–86.
- Cahoon, L. B., Nearhoof, J. E., and Tilton, C. L. (1999). Sediment grain size effect on benthic microalgal biomass in shallow aquatic ecosystems. *Estuaries* 22, 735–741. doi: 10.2307/1353106
- Cahoon, L. B., and Safi, K. A. (2002). Distribution and biomass of benthic microalgae in Manukau Harbour, New Zealand. *New Zeal. J. Mar. Freshw. Res.* 36, 257–266. doi: 10.1080/00288330.2002.9517084
- Cartaxana, P., Mendes, C. R., Van Leeuwe, M. A., and Brotas, V. (2006). Comparative study on microphytobenthic pigments of muddy and sandy intertidal sediments of the Tagus estuary. *Estuar. Coast. Shelf Sci.* 66, 225–230. doi: 10.1016/j.ecss.2005.08.011
- Cartaxana, P., Ruiivo, M., Hubas, C., Davidson, I., Seródio, J., and Jesus, B. (2011). Physiological versus behavioral photoprotection in intertidal epipellic

- and epipsammic benthic diatom communities. *J. Exp. Mar. Bio. Ecol.* 405, 120–127. doi: 10.1016/j.jembe.2011.05.027
- Chen, J., Wang, D., Li, Y., Yu, Z., Chen, S., Hou, X., et al. (2020). The carbon stock and sequestration rate in tidal flats from coastal China. *Glob. Biogeochem. Cycles* 34:e2020GB006772. doi: 10.1029/2020GB006772
- Chen, Y., Dong, J., Xiao, X., Zhang, M., Tian, B., Zhou, Y., et al. (2016). Land claim and loss of tidal flats in the Yangtze Estuary. *Sci. Rep.* 6:24018. doi: 10.1038/srep24018
- Colijn, F., and de Jonge, V. (1984). Primary production of microphytobenthos in the Ems-Dollard Estuary. *Mar. Ecol. Prog. Ser.* 14, 185–196. doi: 10.3354/meps014185
- Consalvey, M., Paterson, D. M., and Underwood, G. J. C. (2004). The ups and downs of life in a benthic biofilm: migration of benthic diatoms. *Diatom Res.* 19, 181–202. doi: 10.1080/0269249X.2004.9705870
- Dalu, T., Cuthbert, R. N., Chavalala, T. L., Froneman, P. W., and Wasserman, R. J. (2020). Assessing sediment particle-size effects on benthic algal colonisation and total carbohydrate production. *Sci. Total Environ.* 710:136348. doi: 10.1016/j.scitotenv.2019.136348
- Davidson, N. C., and Finlayson, C. M. (2019). Updating global coastal wetland areas presented in Davidson and Finlayson (2018). *Mar. Freshw. Res.* 70, 1195–1200. doi: 10.1071/MF19010
- Davis, M., and McIntire, C. (1983). Effects of physical gradients on the production dynamics of sediment-associated algae. *Mar. Ecol. Prog. Ser.* 13, 103–114. doi: 10.3354/meps013103
- Davoult, D., Migné, A., Créach, A., Gévaert, F., Hubas, C., Spilmont, N., et al. (2009). Spatio-temporal variability of intertidal benthic primary production and respiration in the western part of the Mont Saint-Michel Bay (Western English Channel, France). *Hydrobiologia* 620, 163–172. doi: 10.1007/s10750-008-9626-3
- De Jonge, V. N., and Van Beuselom, J. E. E. (1992). Contribution of resuspended microphytobenthos to total phytoplankton in the EMS estuary and its possible role for grazers. *Netherlands J. Sea Res.* 30, 91–105. doi: 10.1016/0077-7579(92)90049-K
- Drylie, T. P., Lohrer, A. M., Needham, H. R., Bulmer, R. H., and Pilditch, C. A. (2018). Benthic primary production in emerged intertidal habitats provides resilience to high water column turbidity. *J. Sea Res.* 142, 101–112. doi: 10.1016/j.seares.2018.09.015
- Du, G. Y., Son, M., Yun, M., An, S., and Chung, I. K. (2009). Microphytobenthic biomass and species composition in intertidal flats of the Nakdong River estuary, Korea. *Estuar. Coast. Shelf Sci.* 82, 663–672. doi: 10.1016/j.ecss.2009.03.004
- Ehrenhauss, S., Witte, U., Janssen, F., and Huettel, M. (2004). Decomposition of diatoms and nutrient dynamics in permeable North Sea sediments. *Cont. Shelf Res.* 24, 721–737. doi: 10.1016/j.csr.2004.01.002
- Eisenhauer, N., Bowker, M. A., Grace, J. B., and Powell, J. R. (2015). From patterns to causal understanding: structural equation modeling (SEM) in soil ecology. *Pedobiologia* 58, 65–72. doi: 10.1016/j.pedobi.2015.03.002
- Ellis, J., Ysebaert, T., Hume, T., Norkko, A., Bult, T., Herman, P., et al. (2006). Predicting macrofaunal species distributions in estuarine gradients using logistic regression and classification systems. *Mar. Ecol. Prog. Ser.* 316, 69–83. doi: 10.3354/meps316069
- Geider, R., Piatt, T., and Raven, J. (1986). Size dependence of growth and photosynthesis in diatoms: a synthesis. *Mar. Ecol. Prog. Ser.* 30, 93–104. doi: 10.3354/meps030093
- Golterman, H. L. (ed.) (1975). “Algae and their pigments,” in *Physiological Limnology: An Approach to the Physiology of Lake Ecosystems*, (Amsterdam: Elsevier Scientific Publishing Company), 233–247.
- Grace, J. B., and Bollen, K. A. (2008). Representing general theoretical concepts in structural equation models: the role of composite variables. *Environ. Ecol. Stat.* 15, 191–213. doi: 10.1007/s10651-007-0047-7
- Guarini, J.-M., Chauvaud, L., and Coston-Guarini, J. (2008). Can the intertidal benthic microalgal primary production account for the “Missing Carbon Sink”? *J. Oceanogr. Res. Data* 1, 13–19. doi: 10.3354/meps071013
- Haro, S., Lara, M., Laiz, I., González, C. J., Bohórquez, J., Garcia-Robledo, E., et al. (2020). Microbenthic net metabolism along intertidal gradients (Cadiz Bay, SW Spain): spatio-temporal patterns and environmental factors. *Front. Mar. Sci.* 7:39. doi: 10.3389/fmars.2020.00039
- Haubois, A. G., Sylvestre, F., Guarini, J. M., Richard, P., and Blanchard, G. F. (2005). Spatio-temporal structure of the epipellic diatom assemblage from an intertidal mudflat in Marennes-Oléron Bay, France. *Estuar. Coast. Shelf Sci.* 64, 385–394. doi: 10.1016/j.ecss.2005.03.004
- Hsieh, H. L., and Chang, K. H. (1991). Habitat characteristics and occurrence of the spionid *Pseudopolydora* sp on the tube-caps of the onuphid *Diopatra bilobata* (Polychaeta: Spionidae Onuphidae). *Bull. Inst. Zool. Acad. Sin.* 30, 331–339.
- Hubas, C., and Davoult, D. (2006). Does seasonal proliferation of *Enteromorpha* sp. affect the annual benthic metabolism of a small macrotidal estuary? (Roscoff Aber Bay, France). *Estuar. Coast. Shelf Sci.* 70, 287–296. doi: 10.1016/j.ecss.2006.06.019
- Hubas, C., Davoult, D., Cariou, T., and Artigas, L. F. (2006). Factors controlling benthic metabolism during low tide along a granulometric gradient in an intertidal bay (Roscoff Aber Bay, France). *Mar. Ecol. Prog. Ser.* 316, 53–68. doi: 10.3354/meps316053
- Hubas, C., Lamy, D., Artigas, L. F., and Davoult, D. (2007). Seasonal variability of intertidal bacterial metabolism and growth efficiency in an exposed sandy beach during low tide. *Mar. Biol.* 151, 41–52. doi: 10.1007/s00227-006-0446-6
- Jassby, A. D., and Platt, T. (1976). Mathematical formulation of the relationship between photosynthesis and light for phytoplankton. *Limnol. Oceanogr.* 21, 540–547. doi: 10.4319/lo.1976.21.4.0540
- Jeffrey, S. W., and Humphrey, G. F. (1975). New spectrophotometric equations for determining chlorophylls *a*, *b*, *c1* and *c2* in higher plants, algae and natural phytoplankton. *Biochem. Physiol. Pflanz.* 167, 191–194. doi: 10.1016/S0015-3796(17)30778-3
- Jenkins, D., and Medsker, L. L. (1964). Brucine method for determination of nitrate in ocean, estuarine, and fresh waters. *Anal. Chem.* 36, 610–612. doi: 10.1021/ac60209a016
- Junoy, J., Castellanos, C., Viéitez, J. M., De La Huz, M. R., and Lastra, M. (2005). The macroinfauna of the Galician sandy beaches (NW Spain) affected by the Prestige oil-spill. *Mar. Pollut. Bull.* 50, 526–536. doi: 10.1016/j.marpolbul.2004.11.044
- Koh, C. H., and Kim, J. S. (2014). The Korean tidal flat of the Yellow Sea: physical setting, ecosystem and management. *Ocean Coast. Manag.* 102, 398–414. doi: 10.1016/j.ocecoaman.2014.07.008
- Laviale, M., Barnett, A., Ezequiel, J., Lepetit, B., Frankenbach, S., Méléder, V., et al. (2015). Response of intertidal benthic microalgal biofilms to a coupled light-temperature stress: evidence for latitudinal adaptation along the Atlantic coast of Southern Europe. *Environ. Microbiol.* 17, 3662–3677. doi: 10.1111/1462-2920.12728
- Lee, L.-H., Hsieh, L.-Y., and Lin, H.-J. (2011). In situ production and respiration of the benthic community during emersion on subtropical intertidal sandflats. *Mar. Ecol. Prog. Ser.* 441, 33–47. doi: 10.3354/meps09362
- Lee, L.-H., and Lin, H.-J. (2013). Effects of an oil spill on benthic community production and respiration on subtropical intertidal sandflats. *Mar. Pollut. Bull.* 73, 291–299. doi: 10.1016/j.marpolbul.2013.05.006
- Lefcheck, J. S. (2016). piecewiseSEM: piecewise structural equation modelling in R for ecology, evolution, and systematics. *Methods Ecol. Evol.* 7, 573–579. doi: 10.1111/2041-210X.12512
- Lin, W.-J., Wu, J., and Lin, H.-J. (2020). Contribution of unvegetated tidal flats to coastal carbon flux. *Glob. Chang. Biol.* 26, 3443–3454. doi: 10.1111/gcb.15107
- McIntyre, H. L., Geider, R. J., and Miller, D. C. (1996). Microphytobenthos: the ecological role of the “Secret Garden” of unvegetated, shallow-water marine habitats. I. Distribution, abundance and primary production. *Estuaries* 19, 185–201.
- McMinn, A., Hirawake, T., Hamaoka, T., Hattori, H., and Fukuchi, M. (2005). Contribution of benthic microalgae to ice covered coastal ecosystems in northern Hokkaido, Japan. *J. Mar. Biol. Assoc. U.K.* 85, 283–289. doi: 10.1017/S0025315405011173h
- Migné, A., Davoult, D., Spilmont, N., Menu, D., Boucher, G., Gattuso, J. P., et al. (2002). A closed-chamber CO₂-flux method for estimating intertidal primary production and respiration under emersed conditions. *Mar. Biol.* 140, 865–869. doi: 10.1007/s00227-001-0741-1
- Migné, A., Davoult, D., Spilmont, N., Ouisse, V., and Boucher, G. (2016). Spatial and temporal variability of CO₂ fluxes at the sediment-air interface in a tidal flat of a temperate lagoon (Arcachon Bay, France). *J. Sea Res.* 109, 13–19. doi: 10.1016/j.seares.2016.01.003

- Migné, A., Spilmont, N., Boucher, G., Denis, L., Hubas, C., Janquin, M. A., et al. (2009). Annual budget of benthic production in Mont Saint-Michel Bay considering cloudiness, microphytobenthos migration, and variability of respiration rates with tidal conditions. *Cont. Shelf Res.* 29, 2280–2285. doi: 10.1016/j.csr.2009.09.004
- Migné, A., Spilmont, N., and Davoult, D. (2004). In situ measurements of benthic primary production during emersion: seasonal variations and annual production in the Bay of Somme (eastern English Channel, France). *Cont. Shelf Res.* 24, 1437–1449. doi: 10.1016/j.csr.2004.06.002
- Murphy, J., and Riley, J. P. (1962). A modified single solution method for the determination of phosphate in natural waters. *Anal. Chim. Acta* 27, 31–36. doi: 10.1057/9781137461131
- Murphy, M. (2020). *semEff: Automatic Calculation of Effects for Piecewise Structural Equation Models Version 0.5.0*.
- Murray, N. J., Phinn, S. R., Clemens, R. S., Roelfsema, C. M., and Fuller, R. A. (2012). Continental scale mapping of tidal flats across east Asia using the landsat archive. *Remote Sens.* 4, 3417–3426. doi: 10.3390/rs4113417
- Murray, N. J., Phinn, S. R., DeWitt, M., Ferrari, R., Johnston, R., Lyons, M. B., et al. (2019). The global distribution and trajectory of tidal flats. *Nature* 565, 222–225. doi: 10.1038/s41586-018-0805-8
- Otani, S., and Endo, T. (2019). “Blue carbon in shallow coastal ecosystems,” in *Blue Carbon in Shallow Coastal Ecosystems*, eds T. Kuwae and M. Hori (Singapore: Springer), 223–250.
- Pai, S.-C., Tsau, Y.-J., and Yang, T.-I. (2001). pH and buffering capacity problems involved in the determination of ammonia in saline water using the indophenol blue spectrophotometric method. *Anal. Chim. Acta* 434, 209–216. doi: 10.1016/S0003-2670(01)00851-0
- Piepenburg, D., Blackburn, T. H., vonDorrien, C. F., Gutt, J., Hall, P. O., Hulth, S., et al. (1995). Partitioning of benthic community respiration in the Arctic (northwestern Barents Sea). *Mar. Ecol. Prog. Ser.* 118, 199–214. doi: 10.3354/meps118199
- Pratt, D. R., Lohrer, A. M., Pilditch, C. A., and Thrush, S. F. (2014). Changes in ecosystem function across sedimentary gradients in estuaries. *Ecosystems* 17, 182–194. doi: 10.1007/s10021-013-9716-6
- Pratt, D. R., Pilditch, C. A., Lohrer, A. M., Thrush, S. F., and Kraan, C. (2015). Spatial distributions of grazing activity and microphytobenthos reveal scale-dependent relationships across a sedimentary gradient. *Estuaries Coasts* 38, 722–734. doi: 10.1007/s12237-014-9857-7
- R Core Team (2021). *R: A Language and Environment for Statistical Computing*. Vienna: R Foundation for Statistical Computing.
- Rahman, M. A., and Ishiga, H. (2012). Trace metal concentrations in tidal flat coastal sediments, Yamaguchi Prefecture, southwest Japan. *Environ. Monit. Assess.* 184, 5755–5771. doi: 10.1007/s10661-011-2379-x
- Sarker, J., Yamamoto, T., and Hashimoto, T. (2009). Contribution of benthic microalgae to the whole water algal biomass and primary production in Suo Nada, the Seto Inland Sea, Japan. *J. Oceanogr.* 65, 311–323. doi: 10.1007/s10872-009-0029-5
- Savelli, R., Bertin, X., Orvain, F., Gernez, P., Dale, A., Coulombier, T., et al. (2019). Impact of chronic and massive resuspension mechanisms on the microphytobenthos dynamics in a temperate intertidal mudflat. *J. Geophys. Res. Biogeosciences* 124, 3752–3777. doi: 10.1029/2019JG005369
- Shiu, J.-W. (2009). *Spatio-Temporal Changes in Biomass and Abundance of Benthic Diatoms in the Kaomei Wetland*. Taichung: National Chung Hsing University.
- Spilmont, N., Davoult, D., and Migné, A. (2006). Benthic primary production during emersion: in situ measurements and potential primary production in the Seine Estuary (English Channel, France). *Mar. Pollut. Bull.* 53, 49–55. doi: 10.1016/j.marpolbul.2005.09.016
- Spilmont, N., Migné, A., Seuront, L., and Davoult, D. (2007). Short-term variability of intertidal benthic community production during emersion and the implication in annual budget calculation. *Mar. Ecol. Prog. Ser.* 333, 95–101. doi: 10.3354/meps333095
- Taguchi, S. (1976). Relationship between photosynthesis and cell size of marine diatoms. *J. Phycol.* 12, 185–189. doi: 10.1111/j.1529-8817.1976.tb00499.x
- Thrush, S. F., Hewitt, J. E., Norkko, A., Nicholls, P. E., Funnell, G. A., and Ellis, J. I. (2003). Habitat change in estuaries: predicting broad-scale responses of intertidal macrofauna to sediment mud content. *Mar. Ecol. Prog. Ser.* 263, 101–112. doi: 10.3354/meps263101
- Tweedie, M. C. K. (1984). “An index which distinguishes between some important exponential families,” in *Statistics: Applications and New Directions. Proceedings of the Indian Statistical Institute Golden Jubilee International Conference*, eds J. K. Ghosh and J. Roy (Calcutta: Indian Statistical Institute), 579–604.
- Underwood, G. J. C., and Barnett, M. (2006). “What determines species composition in microphytobenthic biofilms?” in *Functioning of Microphytobenthos In Estuaries*, eds J. Kromkamp, J. F. C. de Brouwer, G. F. Blanchard, R. M. Forster, and V. Créach (Amsterdam: Royal Netherlands Academy of Arts and Sciences), 121–138.
- Underwood, G. J. C., and Kromkamp, J. (1999). Primary production by phytoplankton and microphytobenthos in estuaries. *Adv. Ecol. Res.* 29, 93–153. doi: 10.1016/s0065-2504(08)60192-0
- Watermann, F., Hillebrand, H., Gerdes, G., Krumbein, W. E., and Sommet, U. (1999). Competition between benthic cyanobacteria and diatoms as influenced by different grain sizes and temperatures. *Mar. Ecol. Prog. Ser.* 187, 77–87. doi: 10.3354/meps187077
- Yoshino, K., Tsugeki, N. K., Amano, Y., Hayami, Y., Hamaoka, H., and Omori, K. (2012). Intertidal bare mudflats subsidize subtidal production through outwelling of benthic microalgae. *Estuar. Coast. Shelf Sci.* 109, 138–143. doi: 10.1016/j.ecss.2012.05.021
- Yu, O. H., Lee, H. G., Shim, W. J., Kim, M., and Park, H. S. (2013). Initial impacts of the Hebei Spirit oil spill on the sandy beach macrobenthic community west coast of Korea. *Mar. Pollut. Bull.* 70, 189–196. doi: 10.1016/j.marpolbul.2013.02.035
- Zhang, R., Zhou, L., Zhang, F., Ding, Y., Gao, J., Chen, J., et al. (2013). Heavy metal pollution and assessment in the tidal flat sediments of Haizhou Bay, China. *Mar. Pollut. Bull.* 74, 403–412. doi: 10.1016/j.marpolbul.2013.06.019

Conflict of Interest: The authors declare that the research was conducted in the absence of any commercial or financial relationships that could be construed as a potential conflict of interest.

Copyright © 2021 Lin, Chiu, Lin and Lin. This is an open-access article distributed under the terms of the Creative Commons Attribution License (CC BY). The use, distribution or reproduction in other forums is permitted, provided the original author(s) and the copyright owner(s) are credited and that the original publication in this journal is cited, in accordance with accepted academic practice. No use, distribution or reproduction is permitted which does not comply with these terms.